

Coherent Topological Charge Structure in CP^{N-1} Models and QCD

Saeed Ahmad¹, Jonathan T. Lenaghan², and H. B. Thacker¹

¹. *Department of Physics, University of Virginia,*

P.O. Box 400714 Charlottesville, VA 22901-4714

² *American Physical Society, One Research Road,*

Box 9000, Ridge, NY 11961-9000, USA

(Dated: today)

In an effort to clarify the significance of the recent observation of long-range topological charge coherence in QCD gauge configurations, we study the local topological charge distributions in two-dimensional CP^{N-1} sigma models, using the overlap Dirac operator to construct the lattice topological charge. We find long-range sign coherence of topological charge along extended one-dimensional structures in two-dimensional spacetime. We discuss the connection between the long range topological structure found in CP^{N-1} and the observed sign coherence along three-dimensional sheets in four-dimensional QCD gauge configurations. In both cases, coherent regions of topological charge form along membrane-like surfaces of codimension one. We show that the Monte Carlo results, for both two-dimensional and four-dimensional gauge theory, support a view of topological charge fluctuations suggested by Luscher and Witten. In this framework, the observed membranes are associated with boundaries between “k-vacua,” characterized by an effective local value of θ which jumps by $\pm 2\pi$ across the boundary.

I. INTRODUCTION

Lattice studies of topological susceptibility and of the flavor singlet pseudoscalar hairpin correlator in QCD [1] have confirmed the role of topological charge and the axial anomaly in generating a large mass for the η' meson. Nevertheless, the local structure of the topological charge fluctuations responsible for these effects is much less well-understood. The interrelation between topological charge fluctuations, chiral symmetry breaking, and confinement is also obscure. Both confinement and χSB reflect the long range structure of the QCD vacuum, so it is natural to ask whether topological charge fluctuations exhibit any kind of coherent long range structure. Of course, conventional long range order is ruled out by spectral considerations, since the pure glue theory has a large mass gap. The topological charge correlation length is determined by the lightest pseudoscalar glueball mass, which lattice calculations have shown to be well above 2 GeV [2]. Furthermore, as first pointed out by Seiler and Stamatescu [3], in the continuum limit, the Euclidean topological

charge two-point correlator $G(x) = \langle q(x)q(0) \rangle$ is required to be negative for all nonzero separation $|x| \neq 0$ [4]. This is a consequence of reflection positivity, from which it follows that *real, propagating intermediate states (glueballs) give a negative contribution to the Euclidean correlator*. The only positive contribution to the topological susceptibility (as determined from the integrated correlator) comes from a positive contact term at $x = 0$ [3]. In spite of the absence of conventional long-range order in pure-gluon QCD, there are reasons to suspect that a more subtle kind of long range order is present. Specifically, it is clear that the essential properties of the gauge fields responsible for χSB should be manifest in the pure gluon theory, even without internal quark loops. This becomes apparent, for example, if we characterize the gluon field by the eigenvalues of the associated Dirac operator. Even quenched gauge configurations will support Goldstone boson propagation and exhibit a chiral condensate in the form of a finite density of near-zero Dirac eigenmodes (up to quenched chiral log corrections). Thus, the long-range order responsible for χSB is built into the gluon field, in spite of the fact that the pure gluon theory has a very large mass gap.

Until recently, the ability to study topological charge structure numerically in lattice QCD has been hindered by the lack of a well-behaved lattice discretization of the local topological charge density. Ultralocal operators constructed directly from the gauge links are found to exhibit a large amount of short-range noise which obscures any possible long-range coherence. The emergence of exactly chiral lattice Dirac operators and associated Ginsparg-Wilson relations has provided a new and vastly improved calculational approach to topological charge studies. In this approach, the local topological charge density,

$$q(x) = \frac{g^2}{48\pi^2} \text{Tr} F \tilde{F} \quad (1)$$

is calculated not from the link fields, but from the exactly chiral lattice Dirac operator [5]

$$q(x) = \frac{1}{2} \text{Tr} \gamma^5 D \quad (2)$$

where D satisfies GW relations

$$\{\gamma^5, D\} = \bar{a} \times D \gamma^5 D \quad (3)$$

and $\bar{a} \propto$ lattice spacing. This construction of the lattice topological charge density arises in the calculation of the axial $U(1)$ anomaly on the lattice [5]. Unlike the topological charge operator constructed from the gauge field [6], the operator (2) turns out to reveal the coherent structure of the topological charge distribution in Monte Carlo configurations without any need for smoothing or cooling procedures.

Using the overlap construction of topological charge density, a recent study of pure-gluon QCD gauge configurations has provided striking evidence for long range topological charge structure in the form of extended three-dimensional sheets in four-dimensional spacetime [8]. A typical gauge configuration (in a periodic box of about $(1.5fm)^4$) contains two sheets of opposite charge which are everywhere thin and close together, forming a crumpled or folded dipole layer which occupies a large fraction of space-time. A more detailed study of the charge distribution within these sheets [9] has shown that the membrane-like structures are inherently global, in the sense that the topological charge distribution is not concentrated in localized lumps but rather is distributed throughout the coherent sheets. By comparing results for three different lattice spacings, it was also found that the thickness of the sheets scales to zero in the continuum limit, and that the presence of these sheets plays a central role in the appearance of the expected positive contact term in the topological charge correlator. The alternating-sign layered arrangement of the coherent sheets give rise to the negative short-distance power-law behavior expected from the operator product expansion [10].

In this paper, we study the distribution of topological charge in the CP^{N-1} model using the overlap Dirac operator. We find that the topological charge distributions calculated by the overlap method in Monte Carlo generated CP^{N-1} configurations exhibit long range structure which is quite analogous to that observed in four-dimensional QCD. In CP^{N-1} , the structures are effectively one-dimensional regions of coherence in two-dimensional spacetime. We note that in both cases the coherent regions have the dimensionality corresponding to the world volume of a domain wall (i.e. codimension 1), a fact that will play a central role in our theoretical interpretation of the observed structure.

II. TOPOLOGICAL CHARGE IN ASYMPTOTICALLY FREE GAUGE THEORIES

A. Topological Susceptibility and Long Range Order in Chern-Simons Currents

The possibility that the vacuum of pure-gluon QCD possesses a “secret long-range order” associated with topological charge was first explored by Luscher [7], who pointed out that if the topological susceptibility χ_t is nonzero, it implies the presence of a zero-mass pole in the correlator of two Chern-Simons currents. Let us define the *abelian* 3-index Chern-Simons tensor

$$A_{\mu\nu\rho} = -Tr \left(B_\mu B_\nu B_\rho + \frac{3}{2} B_{[\mu} \partial_\nu B_{\rho]} \right) \quad (4)$$

where B_μ is the Yang-Mills gauge potential. We consider the Chern-Simons current that is dual to this tensor,

$$j_\mu^{CS} = \epsilon_{\mu\nu\rho\sigma} A_{\nu\rho\sigma} . \quad (5)$$

Although j_μ^{CS} is not gauge invariant, its divergence is the gauge invariant topological charge density

$$\partial_\mu j_\mu^{CS} = \text{Tr} F \tilde{F} = 32\pi^2 q(x) . \quad (6)$$

Choosing a covariant gauge, $\partial_\mu A_{\mu\nu\rho} = 0$, the correlator of two Chern-Simons currents has the form

$$\langle j_\mu^{CS}(x) j_\nu^{CS}(0) \rangle = \int \frac{d^4 p}{(2\pi)^4} e^{-ip \cdot x} \frac{p_\mu p_\nu}{p^2} G(p^2) . \quad (7)$$

From (6) we see that $G(p^2)$ must have a $p^2 = 0$ pole whose residue is the topological susceptibility,

$$G(p^2) \sim \frac{\chi_t}{p^2} . \quad (8)$$

Of course, this pole does not imply the existence of a physical massless particle, because the Chern-Simons current is not gauge invariant. The gauge invariant topological charge correlator $\langle q(x) q(0) \rangle$ has no pole and remains short range. Note that the $1/p^2$ pole in $G(p^2)$ gives rise to a contact term in the topological charge correlator.

To clarify the nature of the long-range order in 4D Yang-Mills theory, Luscher [7] drew on the analogy with 2-dimensional CP^{N-1} sigma models. The continuum action for the CP^{N-1} model is

$$S = \beta N \int d^2 x (D_\mu \mathbf{z})^\dagger \cdot D_\mu \mathbf{z} , \quad (9)$$

where \mathbf{z} is an N -component complex scalar field subject to the constraint $\mathbf{z}^\dagger \cdot \mathbf{z} = 1$, and the covariant derivative is

$$D_\mu = \partial_\mu + i A_\mu . \quad (10)$$

Here A_μ is a $U(1)$ gauge field, but it is an auxiliary field with no kinetic $F_{\mu\nu}^2$ term. It's equation of motion sets it equal to the flavor-singlet current,

$$A_\mu = J_\mu \quad (11)$$

where

$$J_\mu = \frac{1}{2}i \left(\mathbf{z}^\dagger \partial_\mu \mathbf{z} - (\partial_\mu \mathbf{z})^\dagger \mathbf{z} \right) . \quad (12)$$

The A_μ field can be integrated out to give a theory of self-interacting z -particles. On the other hand, if we integrate out the z 's, the effective low energy Lagrangian for the gauge field includes a dynamically generated kinetic term which arises from closed z -loops. This dynamically generated $F_{\mu\nu}^2$ term gives rise to a confining potential between test $U(1)$ charges, and is also the origin of the $p^2 = 0$ pole in the Chern-Simons current correlator and hence of the nonzero topological susceptibility. The continuum topological charge density operator is defined as

$$q(x) \equiv \frac{1}{2\pi} \epsilon_{\mu\nu} \partial_\mu A_\nu . \quad (13)$$

The CP^{N-1} models possess a $U(1)$ gauge invariance and have many properties in common with 4D QCD. For example, they are classically scale invariant and have classical instanton solutions which, like QCD instantons, are of arbitrary radius. Moreover, the CP^{N-1} models undergo dimensional transmutation via a conformal anomaly, acquiring a mass gap and becoming asymptotically free. The CP^{N-1} analogy was also used by Witten [12] to support the assertion that, in unbroken, asymptotically free gauge theories, classical instantons would “melt” due to quantum fluctuations and are thus irrelevant to topological charge structure in QCD. The arguments in both Refs. [7] and [12] lead to a picture of the QCD vacuum which is in some respects a four-dimensional generalization of Coleman’s original discussion [13] of θ -dependence in the massive Schwinger model, in which the θ parameter appears as a background electric field, and instantons play no role. For the comparison of topological charge structure in two-dimensional $U(1)$ theories with that in QCD, Luscher argued that a precise analogy between the two theories could be made by identifying the Chern-Simons currents, since in both theories, nonvanishing topological susceptibility implies a $p^2 = 0$ pole in the j_μ^{CS} correlator. The crucial observation here is that *the $U(1)$ gauge potential A_μ in the CP^{N-1} model should be identified not with the 4D Yang-Mills gauge potential, but rather with the abelian 3-index Chern-Simons tensor (4)*. Similarly, a Wilson loop in 2D corresponds not to a Wilson loop in 4D but rather, a “Wilson bag”, i.e. an integral of $A_{\mu\nu\rho}$ over the three-dimensional world volume of a membrane-like surface. The surface of this bag separates regions of spacetime which have effective values of θ which differ by 2π (or by fractions of 2π for a fractionally charged bag). Here the effective local value of θ is the analog of the local background electric field in Coleman’s Schwinger model analysis. Just as the worldline of a charged particle in 2D serves

as a domain wall separating vacua with two different values of background electric field, so too does the Wilson bag surface in QCD separate two “k-vacua” with values of θ that differ by integer multiples of 2π .

B. Theta-Dependence in QCD from string/gauge duality

Remarkably, the same physical picture emerges from AdS/CFT duality in the context of Witten’s brane construction of QCD [14]. In this construction, the Wilson bag surface associated with the Chern-Simons tensor corresponds to a wrapped 6-brane in type IIA string theory. (The six brane is wrapped around a compact S_4 , so it looks like a 2-brane or membrane in $3 + 1$ dimensions.) Starting with the string theory on $R_4 \times S_1 \times R_5$, one considers the result of introducing N coincident 4-branes, which are wrapped around the S_1 with supersymmetry breaking boundary conditions. The resulting theory on the branes is thus described (at least at long distances) by a four-dimensional $SU(N)$ Yang-Mills gauge theory without supersymmetry. The origin of the θ term in QCD is a five-dimensional Chern-Simons term on the 4-branes of the form $a \wedge F \wedge F$ where a is the $U(1)$ gauge field that couples to the Ramond-Ramond charge of IIA string theory. When the radius of the compactified dimension is small, this reduces to a four-dimensional theta term $\theta F \wedge F$ where θ is given by the Wilson line of the RR $U(1)$ field around the compact dimension,

$$\theta = \oint a_5 dx_5 . \quad (14)$$

In the brane-induced geometry of the IIA string theory, the compact S_1 goes around the circumference of a two-dimensional disk D which has a black hole singularity at its center. The value of $\theta/2\pi$ given by (14) determines the number of units of R-R flux that are threaded through the singularity. This picture leads to multiple “k-vacuum” states where the local values of θ differ by integer multiples of 2π . Adjacent k-vacua are separated by domain walls (to be identified with Wilson bag surfaces) which are the AdS/CFT dual analog of wrapped 6-branes. The fact that θ jumps by a multiple of 2π when crossing a domain wall (a defining property of the Wilson bag surface integral) follows in the string theory from the quantization of the R-R charge on the 6-brane.

C. Corbino disks, the integer quantum Hall effect, and thin domain walls

The interpretation of the 4D theta term as a dimensionally reduced 5D Chern-Simons term is a central feature of the AdS/CFT view of theta dependence. The general analogy we are pursuing in this paper suggests that we should interpret a θ term in the CP^{N-1} model as a dimensionally

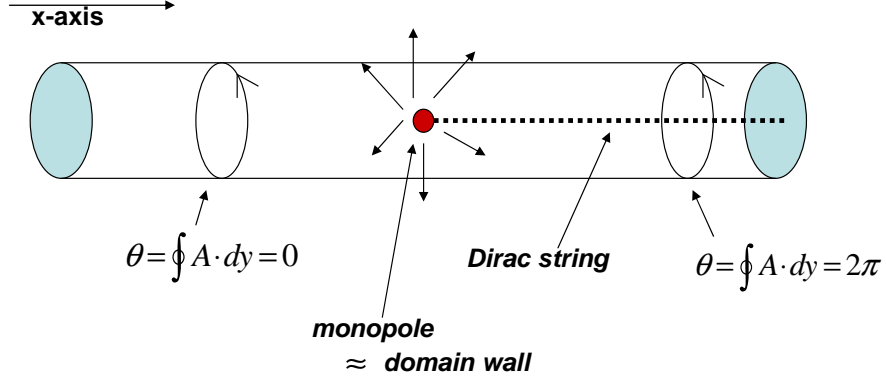


FIG. 1: Holographic view of a domain wall in $(1+1)$ -dimensional CP^{N-1} theories from a $(3+1)$ -dimensional perspective. The long axis of the cylinder becomes the spatial axis of the $(1+1)$ -dimensional theory. Plot is at a fixed time.

reduced three-dimensional Chern-Simons term. In fact, this analogy brings out the deep connection between Witten's description of theta-dependence in Yang-Mills theory [14] and Laughlin's famous topological interpretation of the integer quantum Hall effect [15]. The topology of the $(2+1)$ -dimensional superconductor considered by Laughlin is realized physically by a "Corbino disk," a 2D disk with a hole in it. The Wilson line integral around the disk measures the magnetic flux through the hole. For the purpose of dimensionally reducing this to a $(1+1)$ -dimensional theory with a θ term, it is convenient to consider the topologically equivalent situation of a long thin cylinder, with units of magnetic flux going down the center of the cylinder, as depicted in Figure 1. The quantized flow of Hall current down the length of the cylinder corresponds to a change of θ by an integer multiple of 2π . A domain wall between two different k -vacua along the cylinder is represented in the higher dimensional theory by a magnetic monopole at that location with a Dirac string on one side of it. Note that, in this picture, the transition from, e.g. the $\theta = 0$ vacuum to the $\theta = 2\pi$ vacuum takes place over a distance proportional to the radius of the cylinder, so that in the dimensionally reduced theory, the domain wall becomes infinitely thin. In fact, in the brane construction of QCD, the radius of the compact spatial dimension can be interpreted as a cutoff, somewhat analogous to the lattice spacing in a lattice formulation of the 4D theory. This suggests that, if we interpret the coherent sheets observed in the Monte Carlo simulations as domain wall

boundaries between k-vacua, their thickness should scale to zero linearly with the lattice spacing, i.e. that they should be roughly the same thickness in lattice units, independent of β . This is just what is observed in QCD configurations [10]. As we discuss in Section IV(B), the thickness of the topological charge structures observed in CP^{N-1} also scales to zero linearly in the continuum limit.

D. Wilson Lines, Wilson Bags, and Charge Screening

As emphasized by Witten [12] one should draw a clear distinction between topological charge structure in a spontaneously broken gauge theory (e.g. the 2D $U(1)$ Higgs model) where instantons have a fixed size and are expected to be relevant in the quantum theory, and the structure of an asymptotically free theory such as CP^{N-1} , where the multiple k-vacuum/domain wall picture is expected. Consider a 2D $U(1)$ gauge theory in an infinite volume in which θ is a nonzero constant only on a finite subvolume V , surrounded by a region in which $\theta = 0$, i.e. we add a term to the Euclidean action

$$S \rightarrow S + \int d^2x \theta(x) \epsilon_{\mu\nu} F^{\mu\nu} . \quad (15)$$

where $\theta(x) = \theta$ inside V and $\theta(x) = 0$ outside. Upon integration by parts, such a θ term in the path integral is equivalent to including a Wilson loop around the boundary of V , interpretable as the worldline of a test charge of $\theta/2\pi$ (in units where the charge of the CP^{N-1} field is one),

$$S \rightarrow S + \frac{\theta}{2\pi} \oint_C A \cdot dx \quad (16)$$

where $C = \partial V$.

No matter what the physical mechanism for topological charge fluctuations, we expect the ground state energy to be periodic under $\theta \rightarrow \theta + 2\pi$. However, this periodicity can arise in two physically distinct ways. In a dilute instanton scenario, the topological charge comes in locally quantized lumps which are well enough separated from nearby lumps that we can carve out a local subvolume around a given lump over which the topological charge integrates to an integer ν_i . (We do not consider models involving highly overlapping instantons.) The local quantization of topological charge in an instanton model allows periodicity in θ to be satisfied locally in each small subvolume, since the θ term simply multiplies the partition function by periodic factors $e^{i\theta\nu_i}$ for each instanton. If we change θ continuously from 0 to 2π , we expect smooth periodic behavior without any bulk transition in the vacuum. Expressing the θ term as a Wilson loop around the

boundary, Eq. (16), we can assume that, for a dilute instanton gas, as V gets large, the gauge field in the asymptotic region can be taken to be pure gauge. In this case, the precise location of the Wilson loop has no physical significance. As long as it is in the asymptotic pure-gauge region, it merely counts the number of instantons minus antiinstantons inside V . A much different situation occurs in QCD-like theories where the gauge invariance is unbroken and a finite mass gap arises via quantum effects. In these theories (QCD, discussed in [8] and CP^{N-1} , discussed here), Monte Carlo calculations appear to support Witten's arguments that instantons disappear from the quantum theory and are, in some sense, replaced by domain walls between k -vacua. Topological charge does not appear in locally quantized lumps but rather in extended coherent structures of codimension 1. In this situation, the boundary condition that $F_{\mu\nu} = 0$ asymptotically is not the correct one. If a Wilson loop around V is included in the path integral, it will introduce a physical domain wall separating the $\theta = 0$ vacuum outside from the nonzero- θ vacuum inside. Periodicity in θ arises in a discontinuous way, involving a "string-breaking" or charged pair production process, resulting in the screening or partial screening of the Wilson loop. This is just the mechanism discussed in Coleman's original description of θ -dependence in the massive Schwinger model.

If the topological susceptibility is nonzero, then for generic values of θ , the free energy per unit volume inside V , $E(\theta)$ is greater than $E(0)$, the value outside V . The Wilson loop around V thus satisfies an area law,

$$\langle W(C) \rangle \sim \exp [-(E(\theta) - E(0))V] . \quad (17)$$

This exhibits the linear, confining Coulomb force between test charges of $\pm\theta/2\pi$ at opposite ends of the box. In the two-dimensional case, confinement of $U(1)$ charge and nonvanishing topological susceptibility both arise from the massless pole in the Chern-Simons current correlator. In four-dimensional QCD, the analog of (17) is not confinement of quarks, but rather a "volume law" for Wilson bags:

$$\left\langle \exp \left[i(\theta/2\pi) \int_S A_{\mu\nu\rho} dx^\mu dx^\nu dx^\rho \right] \right\rangle \sim \exp [-(E(\theta) - E(0))V] \quad (18)$$

where S is the surface of a closed bag and V is the enclosed 4-volume. In the two-dimensional theory, as θ is increased the constant electric field between the test charges increases. As θ crosses π , the field becomes strong enough to produce a pair of charged scalars out of the vacuum and send them to opposite ends of the box, screening one unit of electric flux. In the CP^{N-1} model the gauge field is actually an auxiliary field composed of z^+z^- pairs, so it is more accurate to describe the screening process as resulting from a collective motion of the charged z -particles in

the vacuum which leaves a net charge at the two ends of the box. At $\theta = \pi$, the screened and unscreened vacua are degenerate, with the two vacua containing a background of $\pm\frac{1}{2}$ a unit of electric flux. As θ goes through π there is a sudden transition from the unscreened to the screened vacuum. [By contrast, a dilute instanton gas leads to a background electric field $\propto \sin \theta$, which goes smoothly through zero at $\theta = \pi$.] As θ is further increased toward 2π , the energy per unit volume $E(\theta)$ decreases. Finally, at $\theta = 2\pi$ we have $E(2\pi) = E(0)$, and the area term in the Wilson loop vanishes. The external test charge is completely screened by the polarization of the vacuum. At this point there is again no net background flux and no force between the test charges.

A similar discontinuous behavior at $\theta = \pi$ is expected in the case of four-dimensional QCD [7, 12], where the Wilson loop that is used to circumscribe the region of nonzero θ in the two-dimensional theory is replaced by the Wilson bag, which does the same thing in four-dimensional Yang-Mills theory. The force between the bag walls vanishes when the bag has integer charge, i.e. when the step in θ across the bag wall is 2π (or an integer multiple of 2π). This fully screened bag is the gauge theory version of the wrapped 6-brane of IIA string theory. The vanishing of the force between the walls of the bag for $\theta = 2\pi$ is the gauge theory manifestation of the fundamental string theory result, first discovered by Polchinski [16], relating the quantization of Ramond-Ramond charge on a D-brane and the vanishing of the force between two D-branes due to closed string exchange.

In order to discuss topological charge structure in this theoretical framework, we need to determine what the elementary “quasiparticle” excitations of the vacuum are, and what type of topological charge structure is associated with these excitations. Note that we are discussing here the excitations in the flavor singlet channel accessed by the gauge field and topological charge operators, after integrating out the z fields. The spectroscopy of the CP^{N-1} models also includes a multiplet of light nonsinglet mesons (which we use here to define the overall mass gap or relative lattice spacing for different β ’s.) These nonsinglet mesons are the lowest lying physical states in the charge neutral sector. Unlike the singlet channel, the nonsinglet states can be excited by a local $z_i^*(x)z_j(x)$ operator. The spectral structure of the flavor-singlet channel can be discussed in terms of the A_μ correlator, or, equivalently, the Chern-Simons correlator (7). [Because of the constraint $\mathbf{z}^\dagger \cdot \mathbf{z} = 1$, the lowest dimension operator that is available to access the flavor singlet channel is the current (12), which is proportional to A_μ .] Consider the correlator as an analytic function of $s = -p^2$. Since the topological charge correlator $p^2 G(p^2)$ is gauge invariant and there is a mass gap in the theory, it can be asserted that the imaginary part of $p^2 G(p^2)$ is zero below some threshold for real particle production. The threshold is the mass of the lightest flavor-singlet state, which could

be either the mass of a flavor-singlet meson, or (if no stable flavor-singlet meson exists) $s < 4M^2$ where M is the mass of the lightest nonsinglet meson. However, because of the zero mass pole in the Chern-Simons correlator, the imaginary part of $G(p^2)$ includes a zero mass delta function $\propto \delta(s)$. This analytic structure in the gauge correlator for CP^{N-1} models has a close analog in superconductivity theory [17]. In that case, the complex conductivity for any nonzero frequency ω below the mass gap has no absorptive (real) part, due to the absence of resistance. However, because of the purely accelerative mode of the Cooper pairs, the dispersive part has a $1/\omega$ pole, and the absorptive part has a $\delta(\omega)$, representing the DC flow of supercurrent. Because of the presence of the supercurrent, if a charged electron is inserted into a superconductor, the quasiparticle that forms is electrically neutral, corresponding to the electron plus the backflow of the Cooper pairs, which screen the electron charge [18]. The excess charge from the electron ends up on the surface of the superconductor. Thus a quasiparticle excitation in a superconductor is an electrically neutral screened electron. Following this analogy combined with the preceding discussion, we propose that the coherent topological charge excitations observed in CP^{N-1} and QCD should be identified with the screened Wilson loop and the screened Wilson bag, respectively. In the CP^{N-1} case, the screened Wilson line can be interpreted as the world line of a charged z -particle whose Coulomb field has been cancelled out by the backflow of charge in the vacuum. Thus the gauge field associated with an elementary excitation is a one-dimensional thread of A_μ flux which is constant along its length and whose transverse cross-section is a delta-function. On the lattice, this corresponds to the coherent excitation of a single line of links. Recall that the A_μ field is an auxiliary field whose equation of motion sets it equal to the z -particle current, Eq. (11). Thus a Wilson loop excitation can also be interpreted as a filamentary current flow.

In Figure 2 we show the topological charge distribution calculated by the overlap method for a gauge field which consists of a single straight Wilson line excitation. The links along the Wilson line are taken to be a constant nonzero phase, with all other links on the lattice set to unity. The topological charge distribution associated with the Wilson line excitation is a dipole layer, with oppositely charged one-dimensional coherent regions on either side of the Wilson line. This resembles the local structure observed in the Monte Carlo distributions. In a similar way, a Wilson bag excitation of the Chern-Simons tensor which is constant on a 3-surface (and zero elsewhere) in four-dimensional QCD yields a topological charge distribution consisting of oppositely charged coherent three-dimensional regions on either side of the bag surface. Again, this provides a reasonable description of the coherent structure seen in the QCD Monte Carlo distributions.

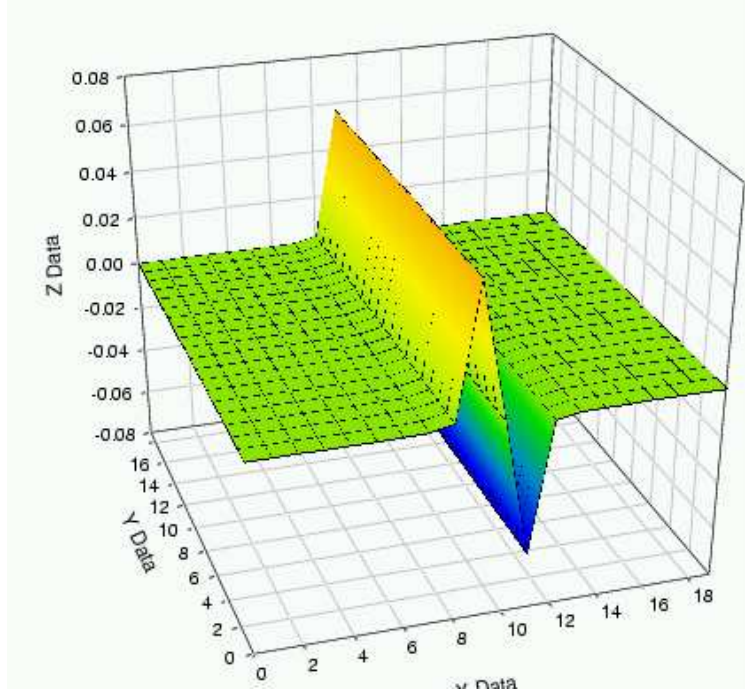


FIG. 2: Plot of the overlap topological charge distribution for a single Wilson line excitation.

III. LATTICE CP^{N-1} MODELS AND MONTE CARLO CALCULATIONS

A. Lattice Action

For the lattice formulation of the CP^{N-1} models, we introduce $U(1)$ link fields $U(x, x + \hat{\mu})$ in the usual way and take the action to consist of gauge invariant nearest-neighbor hopping terms,

$$S = -\beta N \sum_{x, \hat{\mu}} \mathbf{z}(x)^\dagger \cdot \mathbf{z}(x + \hat{\mu}) U(x, x + \hat{\mu}) + c.c. . \quad (19)$$

The naive ultralocal definition of topological charge density on the lattice is in terms of the plaquette phase:

$$q_P(x) = \frac{1}{2\pi i} \log U_P(x) \quad (20)$$

where $U_P(x)$ is the product of phases around a plaquette at site x . Here the principle branch of the log is chosen so that the charge on a plaquette always lies between $-\frac{1}{2}$ and $+\frac{1}{2}$. With toroidal boundary conditions, this definition sums to an integer-valued global topological charge. The analogous construction of topological charge in four-dimensional QCD from gauge variables on the lattice has been given by Luscher [6].

We have found that, just as in four-dimensional QCD, a much better definition of the local topological charge density is given in terms of an exactly chiral overlap Dirac operator D [19]. As shown in [5], if D satisfies Ginsparg-Wilson relations, then the lattice topological charge density operator which appears in the axial $U(1)$ anomaly equation is

$$q(x) = \frac{1}{2} \text{tr} \gamma_5 D(x, x) \quad (21)$$

where the trace is over spin indices in CP^{N-1} and over spin and color indices in QCD. Using the construction of the overlap operator D described in the next section, we have studied topological charge distributions in CP^1 , CP^3 , and CP^9 . We find that the density $q(x)$ defined in (21) reveals the coherent long-range structure that was obscured by the short range noise inherent in the ultralocal operator $q_P(x)$. A detailed comparison of distributions obtained using the overlap q with those obtained using the plaquette operator q_P has been carried out and will be presented elsewhere.

B. Monte Carlo Calculations

The lattice CP^{N-1} action, Eq. (19) was used for Monte Carlo simulation. The updating of the \mathbf{z} fields was done by a Cabibbo-Marinari algorithm consisting of a sequence of $SU(2)$ heat bath updates applied to all possible pairs of z -components. The gauge links were updated by a multi-hit Metropolis algorithm. Calculations were done for CP^1 , CP^3 , and CP^9 . For each value of β , we determine a value for the mass gap by studying the exponential falloff of the $z_i^* z_j$ meson correlator for $i \neq j$,

$$\int dx_2 \langle z_i^* z_j(x) z_j^* z_i(0) \rangle \sim \text{const.} \times e^{-\mu x_1} . \quad (22)$$

The evaluation of μ determines the mass scale. In Table I we give the mass gap μ in lattice units for various values of N and β . The Monte Carlo routine was checked extensively by comparing results with the strong coupling expansion [25] to order β^8 for both the meson correlator and also for the topological charge correlator for the ultralocal $q_P(x)$ operator.

We study lattice volumes up to 50^2 . For each N , values of β were chosen to cover a range of correlation lengths from approximately $\xi = \mu^{-1} = 3$ to 20. Correlator fits were carried out by standard methods, using covariant χ^2 minimization. The statistical errors and autocorrelation times were determined by a bootstrap algorithm.

TABLE I: Massgap in lattice units

β	CP^1	β	CP^3	β	CP^9
1.0	.438(5)	0.8	.554(2)	0.7	.406(2)
1.1	.286(5)	0.9	.327(3)	0.8	.212(2)
1.2	.179(3)	1.0	.180(1)	0.9	.0895(6)
1.3	.111(1)	1.1	.0882(7)	1.0	.0579(2)
1.4	.0696(8)	1.2	.0531(3)	1.1	.0475(4)

C. Overlap Dirac Operator

The overlap construction [19] provides a prescription for constructing an exactly chiral Dirac operator D satisfying the GW relations (3). The construction begins with a suitable ultralocal discretization of the Dirac operator as a kernel. Here we will use the usual Wilson-Dirac operator as the kernel,

$$D_W = \frac{1}{2}\gamma_\mu(\nabla_\mu + \nabla_\mu^*) - \frac{1}{2}a\nabla_\mu^*\nabla_\mu , \quad (23)$$

where ∇_μ and ∇_μ^* are the forward and backward lattice derivatives, respectively,

$$\begin{aligned} \nabla_\mu\psi(x) &= \frac{1}{a}(U_\mu(x)\psi(x+a\hat{\mu}) - \psi(x)) \\ \nabla_\mu^*\psi(x) &= \frac{1}{a}\left(\psi(x) - U_\mu^\dagger(x-a\hat{\mu})\psi(x-a\hat{\mu})\right) . \end{aligned}$$

The overlap operator can be written as

$$D = \frac{1}{a}(1 + \gamma_5 \epsilon(H_W(m))) , \quad (24)$$

where $H_W(m) = \gamma_5 D_W(-m)$ and the sign function is

$$\epsilon(H_W(m)) = \frac{H_W(m)}{\sqrt{H_W^\dagger(m)H_W(m)}} . \quad (25)$$

This operator has a generalized chiral symmetry given by the Ginsparg–Wilson relation

$$\gamma_5 D + D\gamma_5 = \bar{a}D\gamma_5D , \quad (26)$$

as is easily verified.

The Wilson mass parameter can be chosen to lie in the range $0 < m < 2$ with the various values of m giving the same continuum physics. This range is allowed, at least in the case of free fields and for sufficiently smooth gauge field configurations. We have carried out our calculations in the

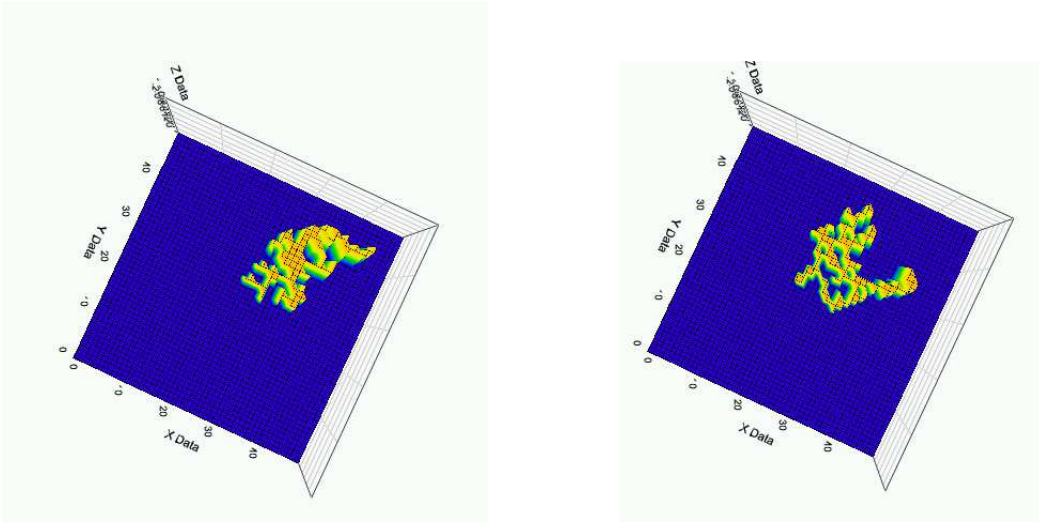


FIG. 3: Two typical largest structures for random $q(x)$ distributions on a 50×50 lattice.

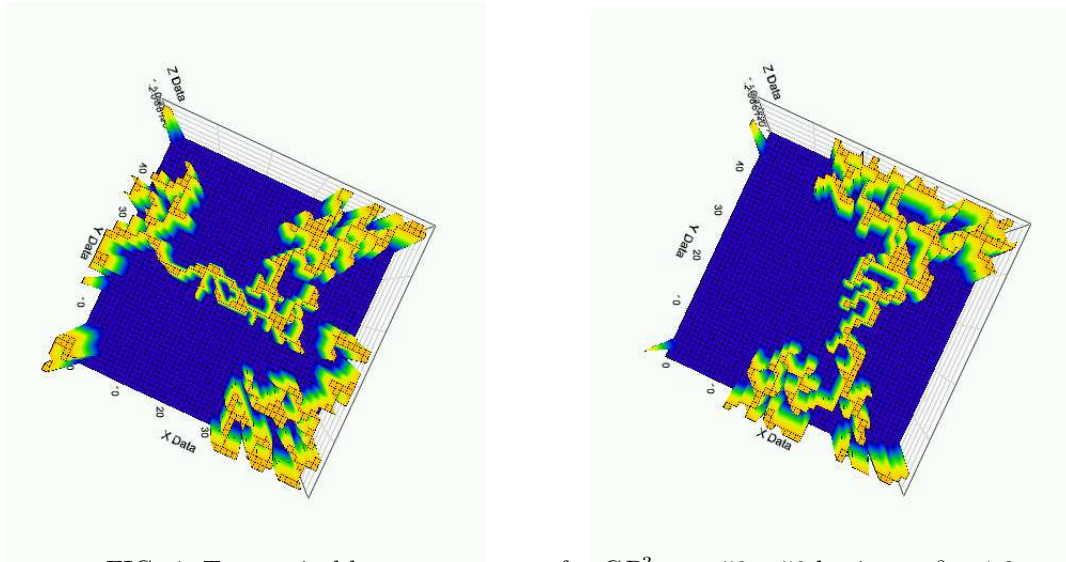


FIG. 4: Two typical largest structures for CP^3 on a 50×50 lattice at $\beta = 1.2$.

range $0 < m < 1$ and found the results to be insensitive to the choice of m in this range. For the lattice sizes used in this study (up to 50×50), it was possible to construct the overlap operator exactly, using a LAPACK singular value decomposition routine. (See [20] for a discussion.)

IV. TOPOLOGICAL CHARGE STRUCTURE IN CP^{N-1} MODELS

Using the overlap definition of the topological charge, visual inspection of the TC distributions for individual configurations reveals well-defined “stringy” patterns in the form of locally one-

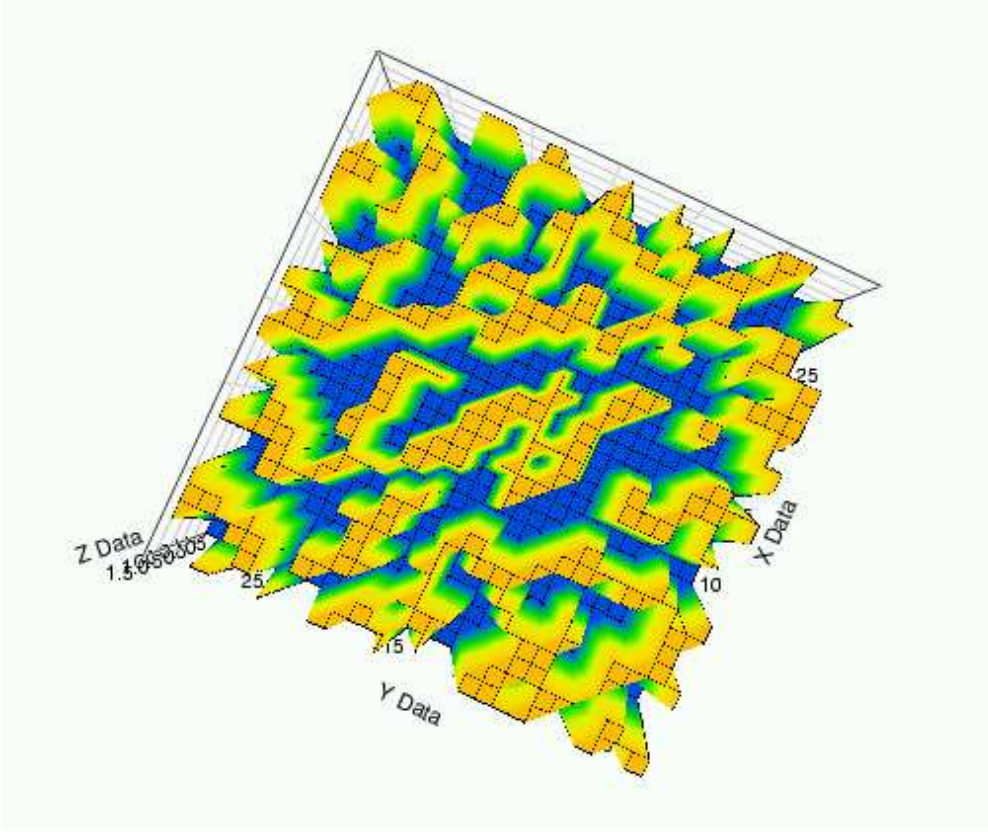


FIG. 5: Plot of the function $\text{sign}(q(x))$ for a CP^3 configuration on a 30×30 lattice at $\beta = 1.2$.

dimensional long range sign coherent structures in the two-dimensional space. These structures are completely analogous to the 3D sheets found in four-dimensional QCD, and precisely what is expected from the Chern-Simons tensor analogy. It is worth pointing out that, when we use the log-plaquette definition of topological charge, we do not observe any such sign coherent structures. [It is interesting to note, however, that much of the qualitative structure seen in the overlap $q(x)$ distribution can also be discerned from the $q_P(x)$ distribution after a simple smoothing procedure, defining the charge at a site to be the average of q_P for the four plaquettes around the site. This comparison will be discussed in detail elsewhere.]

A direct way to get a qualitative view of the coherent topological charge structure in CP^{N-1} is to plot the largest connected structure in each configuration. Here we define a connected structure as a set of nearest-neighbor-contiguous lattice points with the same sign of topological charge. As a reference, we first study the structure plots for randomly generated distributions. Two typical largest structures from a random TC distribution on a 50×50 lattice are shown in Fig. 3. These are to be compared with the structures shown in Fig. 4 which are obtained from the overlap TC distribution for typical CP^3 Monte Carlo configurations at $\beta = 1.2$ (correlation length

≈ 19). Overall, the CP^3 structures are much larger in extent (typically as large as the lattice itself) compared with the random structures. Even more striking is the “stringiness” of the CP^3 structures. They are characterized by long slender regions of coherence which are locally one-dimensional. This contrasts with the random structures which are not only smaller in extent but much more two-dimensional.

Another qualitative feature that can be illustrated graphically is the layered nature of the topological charge distributions, with alternating sign coherent regions interleaved in a somewhat labyrinthine arrangement. Figure 5 shows a plot of $f(x) = \text{sign}(q(x))$ on a CP^3 configuration on a 30×30 lattice. As is the case in QCD, the presence of thin alternating-sign coherent regions of codimension one is in some sense the maximum amount of long range order allowable by the required (and observed) negativity of the correlator for nonzero separation.

To construct a quantitative measure of coherence, we determine the inverse participation ratio (IPR) defined as the inverse fraction of the lattice volume occupied by coherent structures, i.e. $IPR(n) = V/V(n)$, where V is the total volume and $V(n)$ is the volume occupied by n largest coherent structures. (Thus, small localized structures give a large IPR, while a structure occupying most of the lattice would give an IPR close to 1.)

Fig. 6 shows the results for both the overlap $q(x)$ distribution and the log-plaquette operator $q_P(x)$. Also shown for comparison is the same plot for a set of random configurations. These results are from a large ensemble of CP^3 configurations on a 40×40 lattice with $\beta = 1.0$ (correlation length ≈ 5). We see that the overlap definition of $q(x)$ exhibits a clear indication of coherence, e.g. the typical largest structures are much larger than those in a random configuration. Somewhat surprisingly, the plaquette phase definition actually exhibits *less* structure than the purely random distributions. This is an effect of the nearest-neighbor anticorrelation for the plaquette phase.

A. Topological Charge Correlator

In the continuum, the Euclidean topological charge correlator must be negative outside of a positive contact term at $x = 0$. On the lattice, the overlap $q(x)$ is not ultralocal, but it can be argued that it becomes local in the continuum limit, at least for sufficiently smooth gauge fields [7]. Spectral arguments only require the correlator to be negative when the two operators are non-overlapping. The correlator $\langle q(x)q(0) \rangle$ is shown in Figure (8) for CP^3 for several values of β . We see that the correlator consists of a positive core at $x \leq \sqrt{2}$, and a negative short-range tail starting at $x = 2$. Note that the correlator is plotted in lattice units not in physical units. Thus,

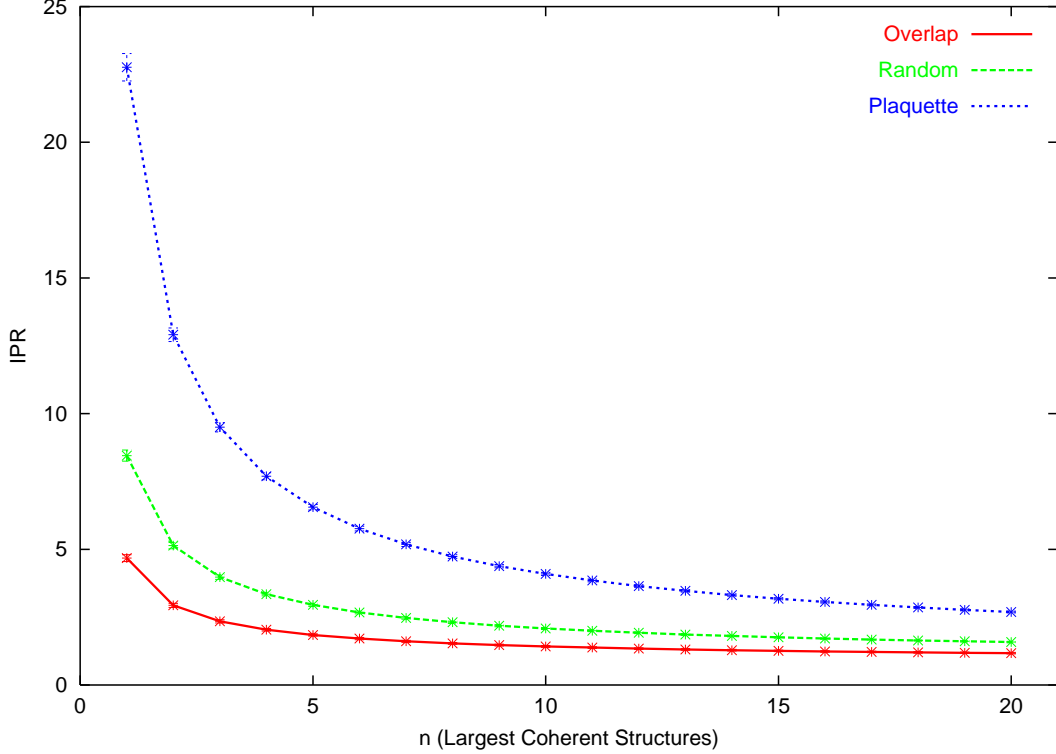


FIG. 6: Inverse participation ratio (IPR) for the overlap and plaquette distributions of the topological charge. For a comparison, we show the result for a random distribution of numbers.

for example, the location of the minimum of the correlator is at $x = 2$ lattice spacings, independent of β . Also, in physical units, the y axis of the plot would be rescaled by a factor of $1/\mu^4$, so the minimum at $x = 2$ is in fact getting much deeper at large β , indicating the development of a short-distance power law singularity.

In Figure (7) we show the separate scaling behavior of the positive and negative contributions to the topological susceptibility, i.e. the integral over $\langle q(x)q(0) \rangle$ for $|x| < 2$ and for $|x| \geq 2$. This shows that the contribution of the contact term and the contribution of the negative tail are separately divergent in the continuum limit, but that the divergence cancels and the topological susceptibility scales nicely. The spatial extent of the positive core region is clearly related to the thickness of the coherent regions, while the negative short-range piece arises from the layered, alternating-sign structure of the configurations.

Figure (9) shows the full topological susceptibility as a function of the mass gap μ for CP^1 , CP^3 , and CP^9 . Here χ_t is plotted in physical units (dividing the lattice value by μ^2), so that a constant value indicates proper scaling behavior. We observe that χ_t appears to be properly scaling with the mass gap for both CP^3 and CP^9 . On the other hand, for CP^1 the topological susceptibility is

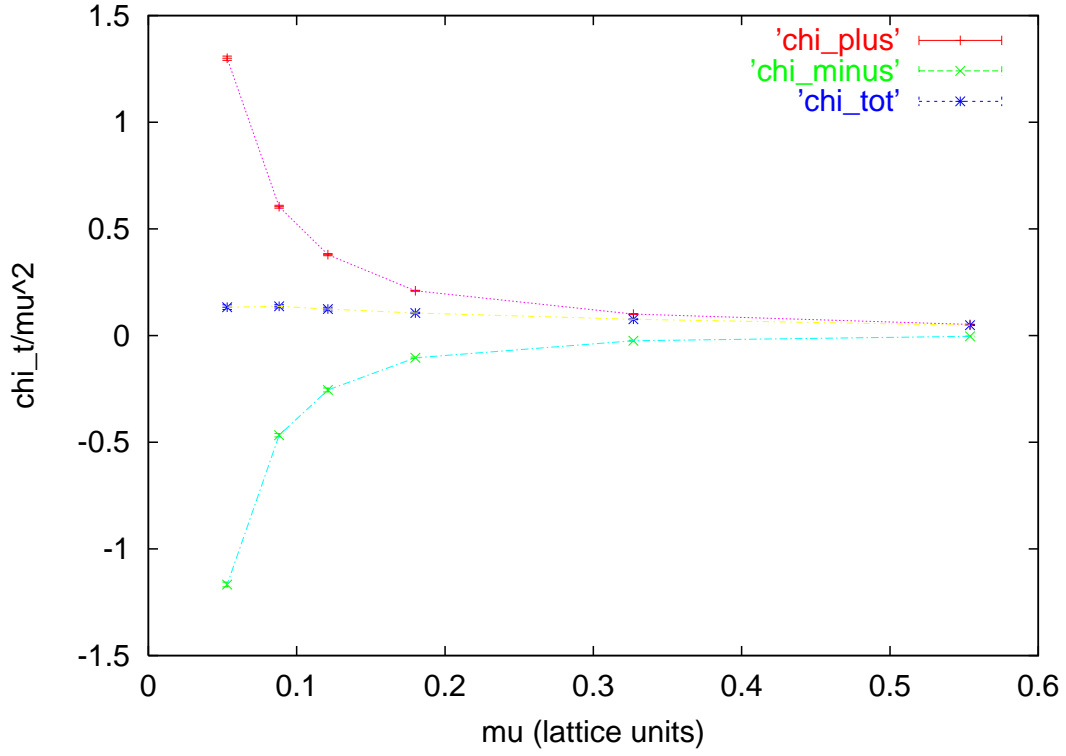


FIG. 7: Scaling behavior of the positive and negative contributions to the topological susceptibility for CP^3

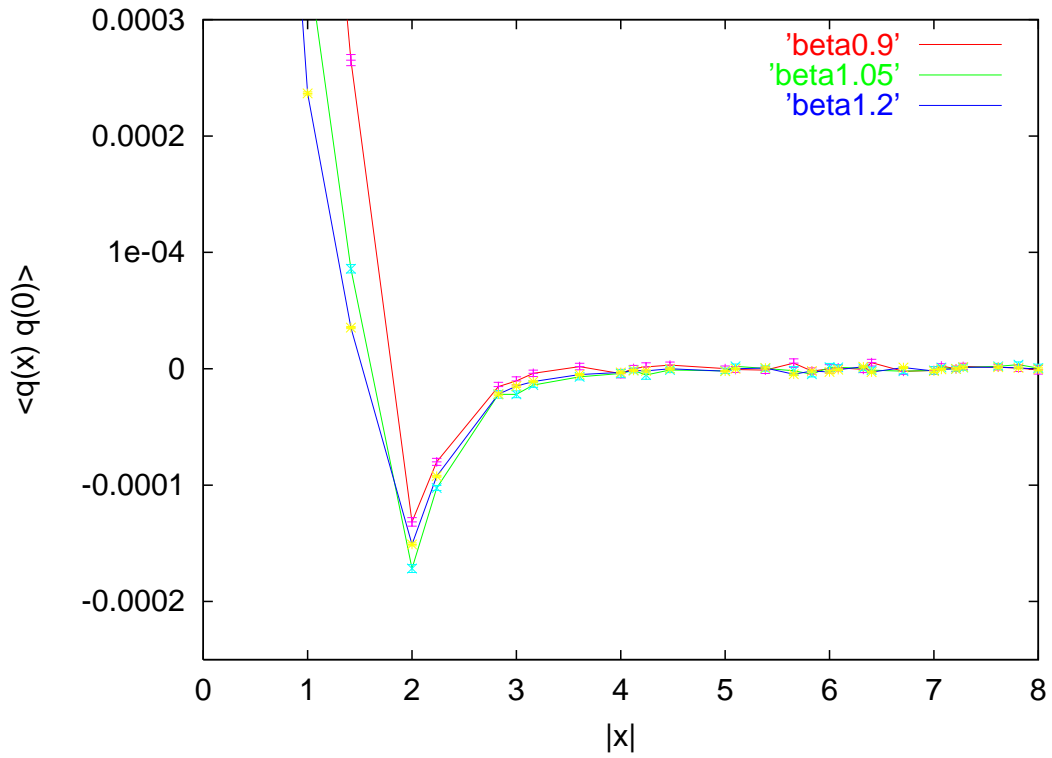


FIG. 8: Topological charge correlator for CP^3 (lattice units).

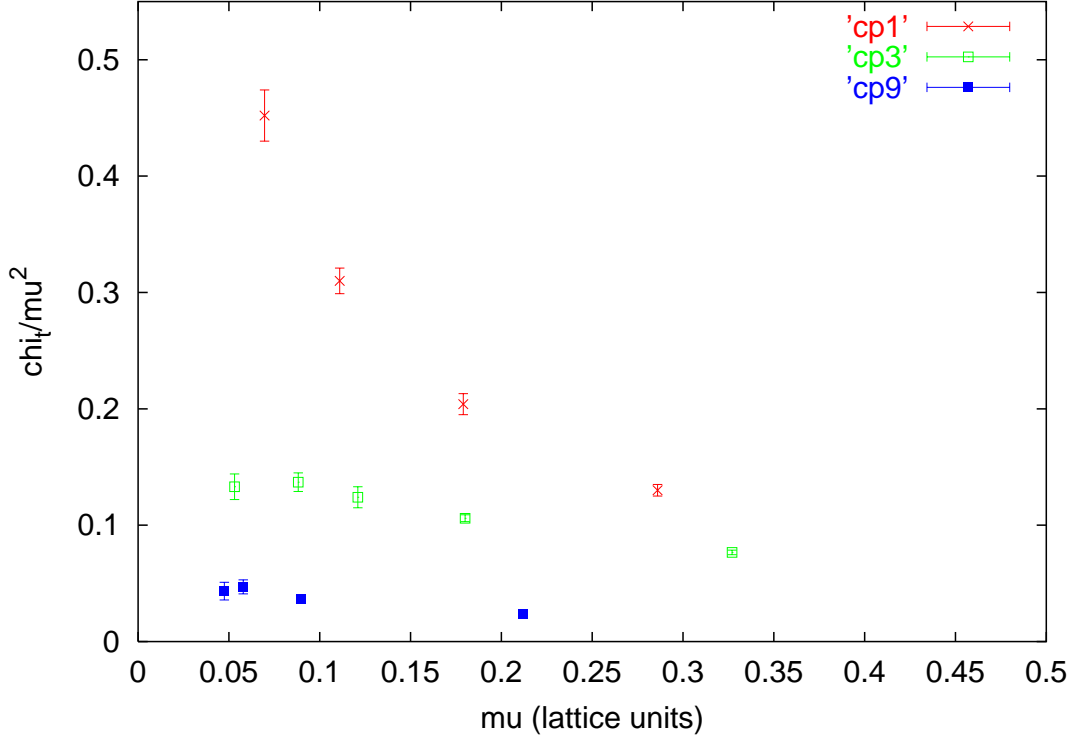


FIG. 9: Scaling behavior of χ_t/μ^2 as a function of inverse correlation length (= mass gap in lattice units) for CP^1 , CP^3 and CP^9

not even approximately scaling. The anomalous scaling behavior of χ_t for CP^1 is believed to be a consequence of the divergent contribution of small instantons with radius of order a [21]. Because of this odd scaling behavior for CP^1 , we have focused most of our structure studies on CP^3 and CP^9 .

B. Thickness of structures

To support the assertion that the size of the positive contact term in the correlator is determined by the thickness of the coherent regions, we can compare this size with a direct measure of the thickness. We calculate the average thickness of a given coherent structure as follows: (1) Choose a particular point on the structure; (2) Walking along a straight path in each of the four directions from that point, measure the length l_{\min} of the shortest path out of the coherent region, i.e. the path to the nearest opposite-sign point; (3) Average over all points on the structure. This length of the shortest path should average to $1/2$ the thickness of the structure, so we define the thickness to be $t = 2\langle l_{\min} \rangle$. Now let us define $x = x_c$ to be the crossover point where the correlator turns from positive to negative. In practice, we have estimated this value by linearly interpolating between

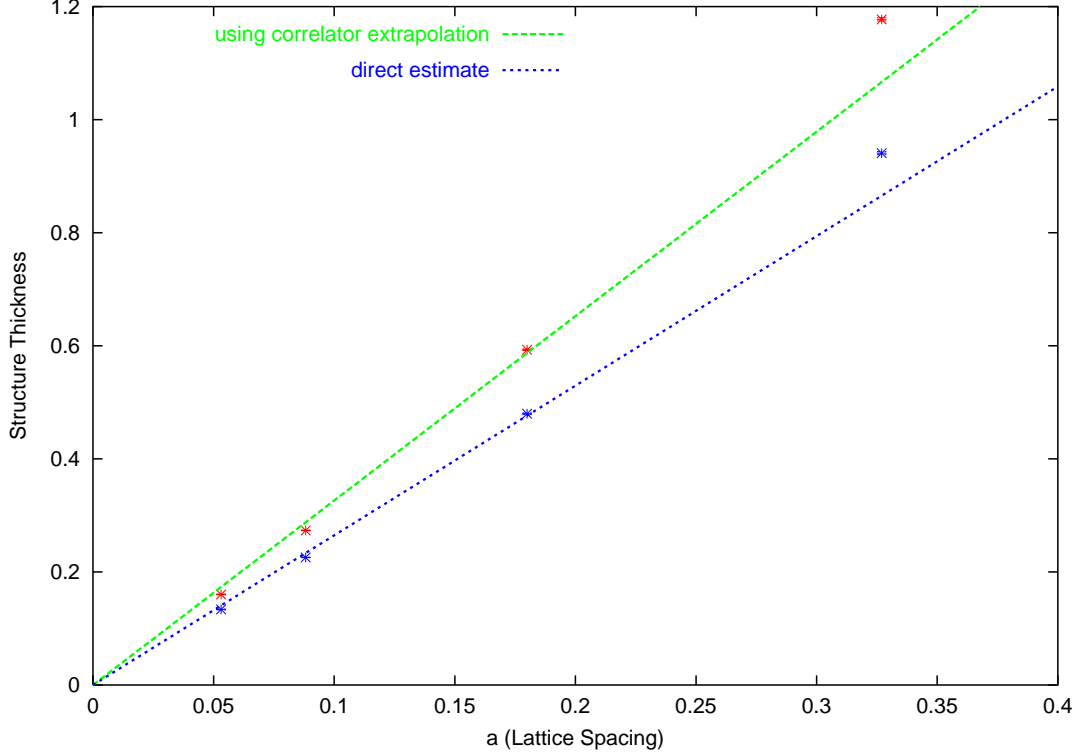


FIG. 10: Physical thickness of the structures as a function of lattice spacing.

the positive value of the correlator at $x = \sqrt{2}$ and the negative value at $x = 2$. If the positive core of the correlator arises from the coherent structures, we might expect that the thickness of the structures would be roughly $2x_c$.

As shown in Figure (10) the direct estimate of the thickness t , and the value obtained from the core size of the correlator are in approximate agreement. Moreover, both of these estimates give a thickness which is approximately constant in lattice units and thus scales to zero linearly in physical units. This agreement leaves little doubt that the positive contact term in the TC correlator arises from the presence of extended, one-dimensionally coherent topological charge structures whose thickness scales to zero in the continuum limit.

C. Hausdorff dimension of structures

To construct another quantitative measure of the effective dimensionality of the largest sign-coherent structures, we computed their Hausdorff dimension. Starting with each site on a structure, we measured the number of other sites $N(r)$ on that structure within a radius r . By fitting $N(r) \propto r^d$, we extract the Hausdorff dimension, d .

Computing the topological charge using the overlap operator, and measuring the Hausdorff

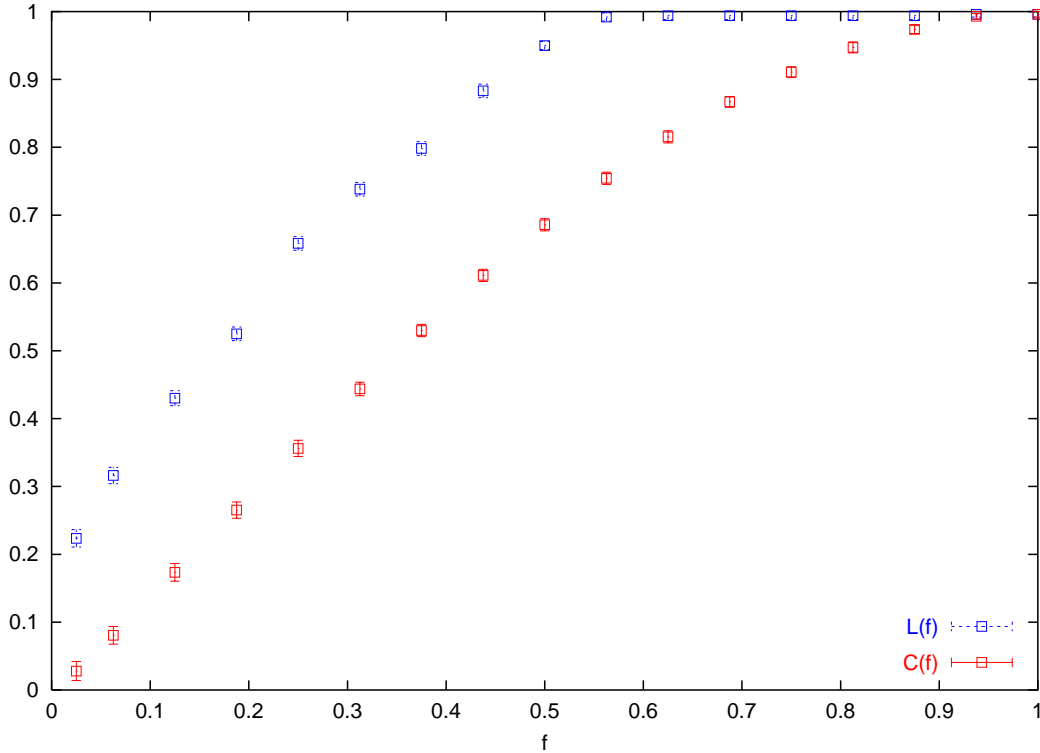


FIG. 11: Variation of $C(f)$ and $L(f)$ as a function of f

dimension of the largest structure in each configuration in the ensemble, we obtain $d = 1.26(6)$, confirming the visual impression that these structures are approximately one-dimensional. For comparison, we studied spin domains in the two-dimensional Ising model just above T_c , adjusted to give structures of the same volume as the CP^{N-1} configurations. The Hausdorff dimension of the Ising spin domains is found to be $d = 1.86(5)$.

D. Inherently Global Nature of the Structures

One result of the QCD studies [9] was that the 3D coherent sheets of topological charge are *inherently global* in structure, in the sense that the topological charge is distributed more or less uniformly throughout the structure and not in localized lumps. A close observation of the CP^{N-1} topological charge distributions reveals that the structures in this case are also inherently global. The 1D structures are, in fact, composed of continuous chains of mountains or valleys of almost constant heights. In other words, the most intense points join together to form the structures. To prove this point quantitatively, we study the variation of the length of the largest structure and the topological susceptibility as a function of the fraction f of points included, starting with the most intense points, as ranked by $|q(x)|$. This type of analysis was applied to the QCD structures

in Ref. [9, 22]. The cumulative function $C(f)$ of the topological susceptibility [9] represents the fraction of the total topological susceptibility obtained when only a fraction f of the most intense points are included in the calculation. It is defined as:

$$C(f) = \frac{\chi(f)}{\chi(1)}; \quad \chi(f) \equiv \frac{\langle Q^2(f) \rangle - \langle Q(f) \rangle^2}{V}; \quad Q(f) = \sum_{x \in S(f)} q(x) \quad (27)$$

where $V \equiv a^2 N$, N being the total number of points on the lattice, and $S(f)$ is the set of points above the threshold introduced via f . The length of a structure is defined as the maximal distance between two points on the structure, i.e. $l(\Gamma) \equiv \{ \max |x - y| : x, y \in \Gamma \}$, where Γ is the set of points lying on the same structure.

The ratio of the length of the largest structure at any fraction f to that at $f = 1$ is $L(f)$, i.e. $L(f) \equiv \frac{l(f)}{l(1)}$. A plot of $C(f)$ and $L(f)$ (see Fig. 11) as a function of f shows that $L(f)$ increases much more rapidly than $C(f)$, and reaches 1 at $f = 0.5$, when only half of the total points are considered on the basis of the intensity criterion. This proves that the most intense points are connected together and the structures are in fact inherently global, in the sense discussed in [9].

V. CONCLUSIONS AND DISCUSSION

In this paper we have presented Monte Carlo results for topological charge structure in two-dimensional CP^{N-1} sigma models. These models exhibit long-range one-dimensionally coherent topological charge structure which is precisely analogous to the three-dimensional coherent sheets observed in four-dimensional pure glue QCD in Reference [8]. The analogy between the two-dimensional $U(1)$ gauge potential A_μ in CP^{N-1} and the *abelian* 3-index Chern-Simons tensor $A_{\mu\nu\sigma}$ in QCD provides a natural framework for interpreting the long range structure in both theories. In this framework, the elementary topological charge excitations of QCD are the “Wilson bags” first suggested by Luscher [7]. A closed Wilson bag in four dimensions is analogous in CP^{N-1} to the creation and annihilation of a $z^+ z^-$ pair, forming a closed Wilson loop.

The alternating-sign layered arrangement of the coherent regions in the Monte Carlo configurations (c.f. Fig. (5)) is a central feature of the topological charge structure in both two-dimensional and four-dimensional theories. At a calculational level, it is clear that this layered structure is enforced by the requirement that, in the continuum, the two-point TC correlator is negative for nonzero separation. An attractive feature of the Wilson bag (Wilson line) as the fundamental topological excitation of QCD (CP^{N-1}) is that the associated topological charge distribution is a dipole layer, which leads naturally to the alternating-sign layering that is observed. The physical

vacuum is presumably a condensate of these surfaces. Both the thickness of the surfaces and the average spacing between adjacent surfaces are going to zero in the continuum limit, leading to the distinctive features of the TC correlator: (1) A positive, divergent contact term, (2) A negative, divergent short distance term, and (3) A cancellation between the (separately divergent) positive and negative contributions to the integrated correlator, giving a finite topological susceptibility which scales properly, $\propto \mu^2$. For the CP^{N-1} case, we can also associate this structure with the fact that the gauge field is an auxiliary field representing a coherent oscillation of charged z -particles. The dynamically generated kinetic term for the gauge field, which arises from closed z -loops, is in fact responsible for the $1/q^2$ pole in the CS correlator and hence is the origin of finite topological susceptibility.

Thus, the picture of the gauge field vacuum as consisting of a dense gas of Wilson line excitations in two-dimensional Euclidean space is apparently compatible with the more familiar view of the CP^{N-1} ground state as a plasma of flavor-singlet z^+z^- pairs which supports the oscillations of the gauge field, generates the $1/q^2$ pole via loop effects, and produces finite topological susceptibility. This latter view is made explicit in the large N solution. Although the model of topological charge excitations based on screened Wilson lines seems to be generally compatible with the large N analysis, the nature of charge screening in the model differs significantly from that which appears in the large N solution. Large N leads to a “quark model” view of both singlet and nonsinglet mesons, which are loosely bound but confined z^+z^- states held together by the linear Coulomb force associated with the dynamically generated $F_{\mu\nu}^2$ term. There would thus be a constant density of topological charge (electric field) between the two constituents of the bound state. One might then expect Euclidean topological charge distributions to be dominated by large coherent two-dimensional bubbles of topological charge, whose thickness was determined by the confinement scale. Not only is this inconsistent with what is seen in the Monte Carlo, but it also would produce a positive TC correlator for distances less than the confinement length, violating the spectral requirement. It has been argued [23, 24] that the large N solution is actually misleading in this regard because the large N saddle-point approximation entails a subtle violation of Elitzur’s theorem. This argument suggests that the nature of the screening of the $U(1)$ charge is more accurately represented by the lattice strong coupling expansion, where it is easily seen that, because of the absence of a bare gauge kinetic term, screening takes place *ultralocally*, in the sense that the only nonvanishing terms are those in which the net current flowing on every link is zero. This phenomenon, which has been referred to as “superconfinement,” strongly suggests that, even in the continuum limit, charge screening should take place locally. The fact that we observe essentially

one-dimensional coherent regions of topological charge, which have a typical thickness proportional to the lattice spacing, appears to support the superconfinement view of charge screening in the CP^{N-1} models. Further Monte Carlo studies of charge screening in the CP^{N-1} models might shed additional light on this issue.

The view of QCD dynamics provided by AdS/CFT holography constitutes a powerful new framework from which to explore the structure of the QCD vacuum [26]. The issue of topological charge structure and θ -dependence in QCD lies at the heart of the AdS/CFT correspondence. As discussed by Witten [14], the string theory dual of QCD topological charge is Ramond-Ramond charge in IIA string theory. This is the fundamental solitonic, or “magnetic” charge of the theory which is not carried by ordinary string states, but is carried by D-branes. Comparing Witten’s discussion of θ -dependence from AdS/CFT holography with the earlier, purely four-dimensional discussion of Luscher [7], it is clear that the “Wilson bag” 3-surface is holographically dual to a wrapped 6-brane in Witten’s description. Both of them have the defining property that the local value of θ jumps by 2π across the surface.

The possibility of directly confronting detailed aspects of the AdS/CFT correspondence with Monte Carlo data is particularly exciting. Ongoing Monte Carlo experiments on the coherent structures in both QCD and CP^{N-1} should provide further, more detailed, tests of the Wilson bag interpretation.

We are grateful to P. Arnold, P. Fendley, and Y. Lian for discussions on these and related topics. This work was supported in part by the Department of Energy under grant DE-FG02-97ER41027.

-
- [1] W. A. Bardeen, A. Duncan, E. Eichten and H. Thacker, Phys. Rev. D **62**, 114505 (2000).
 - [2] G. Bali, Phys. Rept. 343: 1 (2001).
 - [3] E. Seiler and I. O. Stamatescu, MPI-PAE/PTh 10/87.
 - [4] E. Vicari, Nucl. Phys. B554: 301 (1999).
 - [5] P. Hasenfratz, V. Laliena, F. Niedermayer, Phys. Lett. B427, 125 (1998).
 - [6] M. Luscher, Commun. Math. Phys. 85:39 (1982).
 - [7] M. Luscher, Phys. Lett. B78, 465 (1978).
 - [8] I. Horvath et al, Phys. Rev. D68, 114505 (2003).
 - [9] I. Horváth et al, Phys. Lett. B612: 49 (2005).
 - [10] I. Horváth et al, Phys. Lett. B617: 21 (2005).
 - [11] A. Alexandru, I. Horvath, J. Zhang, Phys. Rev. D72:034506 (2005).
 - [12] E. Witten, Nucl. Phys. B149, 285 (1979).

- [13] S. Coleman, *Annals Phys.* 101, 239 (1976).
- [14] E. Witten, *Phys. Rev. D* 81, 2862 (1998).
- [15] R.B. Laughlin, *Phys. Rev. B.* 23, 5632 (1981), *Phys. Rev. Lett.* 50, 1395 (1983).
- [16] J. Polchinski, *Phys. Rev. Lett.* 75, 4724-4727 (1995).
- [17] M. Tinkham, Superconductivity, Documents on Modern Physics, Gordon and Breach, NY, 1965.
- [18] S. A. Kivelson, D. S. Rokhsar, *Phys. Rev. B* 41, 11693-11696 (1990).
- [19] H. Neuberger, *Phys. Rev. Lett.* 81, 4060-4062 (1998).
- [20] L. Giusti, C. Hoelbling and C. Rebbi, *Phys. Rev. D* **64**, 054501 (2001).
- [21] M. Luscher, *Nucl.Phys. B* 200, 61 (1982).
- [22] I. Horvath, *Nucl.Phys. B* 710, 464-484 (2005).
- [23] E. Rabinovici and S. Samuel, *Phys. Lett. B* 101: 323 (1981).
- [24] S. Samuel, *Phys. Rev. D* 28: 2628 (1983).
- [25] N. Seiberg, *Phys. Rev. Lett.* 53: 637 (1984).
- [26] D. Gross and H. Ooguri, *Phys. Rev. D* 58: 106002 (1998).